Original Research

Combining Multi-Indices by Neural Network Model for Estimating Canopy Chlorophyll Content: a Case Study of Interspecies Competition between *Spartina alterniflora* and *Phragmites australis*

Pudong Liu[1], Runhe Shi[2,3,4], Fei Meng[1], Jiantao Liu[1], Guobiao Yao[1], Pingjie Fu[1]*

[1]School of Surveying and Geo-informatics, Shandong Jianzhu University, Jinan, 250101, China
[2]Key Laboratory of Geographic Information Science, Ministry of Education, East China Normal University, Shanghai, 200241, China
[3]Joint Laboratory for Environmental Remote Sensing and Data Assimilation, East China Normal University & Institute of Remote Sensing and Digital Earth, Chinese Academy of Sciences, Shanghai, 200241, China
[4]School of Geographic Sciences, East China Normal University, Shanghai, 200241, China

Abstract

The invasive species *Spartina alterniflora* show a significant coexistence zonation pattern with local *Phragmites australis* in different mixture ratio, increasing the difficulty to monitor their distribution directly by remote sensing. Canopy chlorophyll content (*CCC*) is an important indicator to monitor the growth and physiological status. The objective of this study was to estimate *CCC* under different mixture ratio. Five spectral indices were selected and combined via back propagation (BP) neural network model for estimating *CCC*. Combining multi-indices yielded better results (R^2 = 0.7729, *RMSE* = 53.01 ug.cm^{-2}) on average than the best single spectral index (R^2 = 0.7190, *RMSE* = 63.53 ug.cm^{-2}) without distinguishing interspecies competition, with a total increase of 7.5% in the R^2 and a decrease of 16.56% in the *RMSE*. Meanwhile, when considering interspecies competition, the estimating results obtained by the BP neural network model achieved a further improvement of the R^2 value, ranging from 3.57% to 20.37%, while the prediction error reduced at varying degrees (maximum reduction of 23.78%). The results indicate that combining multi-indices by BP neural network model can alleviate the influence of interspecies competition and achieve higher estimating accuracy.

Keywords: interspecies competition, canopy chlorophyll content, BP neural network, *Spartina alterniflora*, *Phragmites australis*

*e-mail: fupingjie19@sdjzu.edu.cn

Introduction

As one of the three major ecosystems on earth, coastal wetlands are vital and provide many direct or indirect ecosystem service functions, such as the circulation of carbon and nitrogen, and energy transmission, as well as tourism and recreation, which are the cornerstones of regional development [1-3]. However, while coastal wetlands provide various services and products, their continued survival has been threatened in recent decades [4-6]. Invasive species have been increasing in aggravation annually in both scope and spreading speed, thereby contributing to increased pollution and nutrient levels. Invasive plants are one of the most serious threats to ecological global security [7, 8], and plant invasion is an emerging driver of change worldwide. In China, especially in the coastal regions, wetlands are threatened by exotic species that have the ability to alter the native ecosystems, ranging in degree from genetic to ecosystem level [7, 9, 10].

Spartina alterniflora (*S. alterniflora*), one of the most widespread invasive species in China, is native to the North American Atlantic coast and was introduced to Yangtze Estuary in the 1990s [11] little is known regarding the response of functional bacteria involved in the sulfur redox cycling to invasive Spartina alterniflora. We compared community abundance and composition of sulfate reducing bacteria (SRB. *S. alterniflora* has spread rapidly along China's coast for the past 30 years owing to its strong roots and higher tolerance to varying soil conditions than other native salt marsh vegetation [4, 12, 13]. This spread has caused serious ecological consequences to the local ecosystems [9, 14-16]. Furthermore, the invasive species *S. alterniflora* even caused changes in species at the genetic scale, causing serious jeopardize to biodiversity [17]. With the rapid spreading in the Yangtze River Estuary, a large coexistence with the native species, *Phragmites australis* (*P. australis*), has been observed. More importantly, this mixed growing causes competitive interactions along the estuary, causing an unstable distribution as *S. alterniflora* and *P. australis* compete for the limited growing space and nutrient, which we called it interspecies competition in our study. As a region with the most interspecies competition among species, this specific mixed area is important for wetland ecology research. Furthermore, this co-exist region exhibits a sharp changing by mixture ratio, increasing the difficulty to focus on the quantitative estimating for the species using satellite imagery directly. Monitoring this specific mixed growing region are necessary to estuary ecosystem security.

Chlorophyll is an essential biochemical component for plant photosynthesis and the engine of plant growth [18, 19]. Focusing on the photosynthetic characteristics of wetland vegetation is of great significance as it determines the ecological purification effect of the wetland. Canopy chlorophyll content (*CCC*) is of considerable importance because it can indicate the condition for plant growth and physiological status at the canopy level directly [20, 21]. Further, the research on for the estimating of *CCC* is the basis for quantitative inversion domain by remote sensing image. Therefore, information on *CCC* is critical for monitoring the growth situation of *S. alterniflora* and *P. australis,* especially for this specific mixed region. As of late, studies have been focused on vegetation observation and monitoring, and the retrieval of chlorophyll content via non-destructive remote sensing methods, achieving many scientific results [22-27]. Due to the complexity of the radiative transfer model and growth conditions at the canopy level, the estimation of *CCC* has typically been carried out by combing multi-indices that can be found in many cases [28-33]. However, basing on the goal of our research, it is urgent and necessary by focusing on this specific region with the coexistence of these two species for the quantitative estimating of *CCC*.

CCC estimated from remote sensing tends to use empirical statistical [18, 34-36] and physical model inversion [37-41]. Researches have been devoted to excavate sensitive regions that relating to biochemicals by using different combinations of wavelengths measured by different platforms [10, 42-44]. Although various indices for chlorophyll estimation have been established, there is no universal index that is suitable for different species, especially for marsh areas. A single index may be inadequate for estimating the *CCC* in different mixture ratio as it can be easily influenced by the ratio. The growth morphology and vegetation leaf cover can change obviously compared with single pure species, leading the difficulty in quantitative estimating of *S. alterniflora* and *P. australis* at canopy level.

In this research, 46 spectral indices in our database were evaluated for the potentiality of estimating *CCC* under different interspecies mixture ratio between *S. alterniflora* and *P. australis*. Herein, the key study objectives are as follows: (1) determine whether the canopy spectral reflectance are influenced by interspecies competition and (2) determine whether considering interspecies competition can be beneficial for estimating *CCC* and (3) determine if combining multi-indices to estimate the mixed *CCC* alleviates the effect of interspecies competition and improves accuracy. In our research, a control experiment between *S. alterniflora* and *P. australis* is conducted in the field to estimate the *CCC* in the mixed condition, and model simulated data by PROSAIL is used to establish an inversion model under the basis of measured canopy parameters.

Materials and Methods

In our study, we designed a novel experiment and collected samples for the estimating of *CCC*. The experiment details and sampling strategy are shown in the following sections.

Study Sites

Chongming Island, a typical salt marsh wetland located in the Yangtze River Estuary, was selected to conduct our field control experiment owing to the good guarantee conditions of National Bird Nature Reserve. The experiment site was conducted in Dongtan wetland reserve, locating at point A, Shanghai, China (31°38′N, 121°58′E) (Fig. 1). In addition, we also selected field site at the point B (Fig. 1) as the basis for the experimental design. The typical salt marsh wetland of site B is located between North Liuyao and North Bayao of the Yangtze River Estuary with a convenient transportation, which is not affected by artificial embankment. The salt marsh plant in this region was in good growth condition. Herein, the invasive *S. alterniflora* and the native *P. australis* have both large pure species growth zones and large-scale mixed growth areas, which is almost no interference from other species.

Experimental Data Measurements

The control experiment was conducted from early April 2016. The experiment control boxes were stuffed with pure sand, adding with seawater and additional necessary nutrients (Fig. 1A). And the salinity of soil was controlled at 8±1ppt approximately in order to ensure a balanced competitive environment [45, 46]. Then, the *S. alterniflora* and *P. australis* seedlings were collected from the natural field of Chongming Island (Fig. 1B) and transported to the experimental control boxes. In this study, we set the interspecies mixture ratio between *S. alterniflora* and *P. australis* as 3:1, 1:1, 1:3 separately, and two pure species were also conducted as reference controls, and the density of each container was 100 shoots·m^{-2}, which was approximately the same density as the initial wild growth. The experiment was set in five containers per group, repeating three times. We adjusted the salinity once a week and the water levels every 3 d (2 d in the summer) by adding water or salt to maintain salinity concentration to ensure that the initial experimental conditions were maintained throughout the experiment. Note that we mainly focused on the invasive species *S. alterniflora,* four different ratios were selected except pure *P. australis* for the estimation of *CCC* under different mixture ratio in the following research.

Chlorophyll Content Measurements

The sample leaves of *S. alterniflora* and *P. australis* were collected at the experiment site A (Fig. 1A). Sampling leaves were first taken on April 27. For sample selection, a strict accordance with the ecological sample selection rules was conducted. We divided the growing containers into upper and lower leaves, of which ten of each were collected for the different mixture ratio in each container. Then the leaves were immediately sealed into plastic bags and transported to the nearby laboratory, with the temperature keeping at 0ºC. Meanwhile, we used a wet chemical method to extract chlorophyll content. Each sample was put into 95% alcohol for chlorophyll extraction. Next, the samples were macerated in the alcohol labeled in each volumetric flask and maintained in dark conditions for 24 h. Then, the chlorophyll content were calculated using three equations referenced from former published research (see [10] for reference).
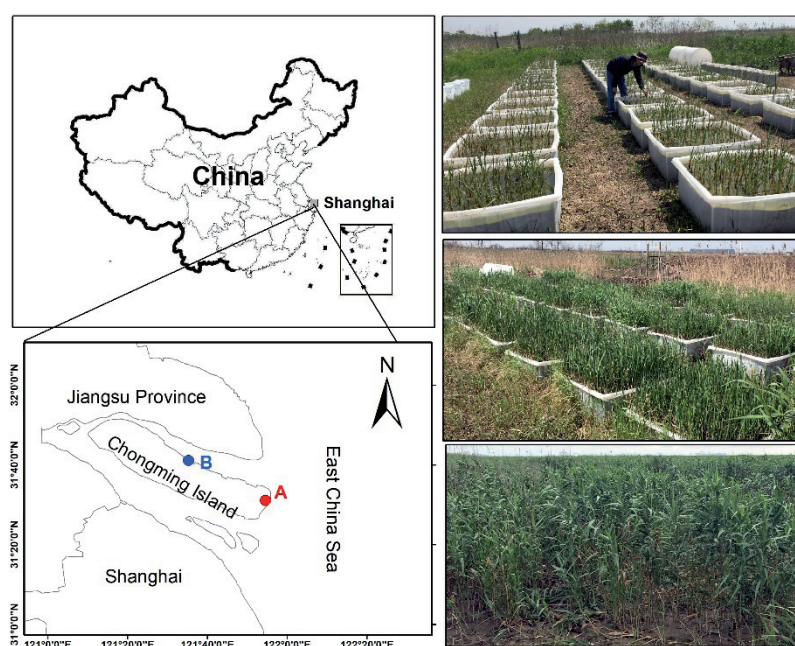

Fig. 1. Location of the study area.

Then, the *CCC* was calculated by the following:

$$Cab_{canopy} = Cab_{leaf} \times LAI \qquad (1)$$

The Cab_{canopy} represents the *CCC*, and Cab_{leaf} represents the leaf chlorophyll content, and the LAI represents the leaf area index. Basing on the calculation, the *CCC* can vary by different interspecies competition.

LAI Measurements

The LAI was measured using the widely used Plant Canopy Analyzer (LAI-2200, LI-COR, Inc., Lincoln, NE, USA) instrument in the early dawn or nightfall around the time of leaf sample collection. The measurements of LAI and chlorophyll content were synchronized in time. This process was strictly conducted and the effect of direct sunlight on the observation results was avoided as much as possible.

Canopy Spectral Reflectance Measurements

The canopy spectral reflectance of each competition ratio container was measured using the ASD FieldSpec HandHeld Portable Spectroradiometer (Analytical Spectral Devices, Boulder, CO, USA) with the assistance of a canopy measurement bracket designed by our group (Fig. 1a) according to the actual field survey and growth containers, we found the average canopy reflectance by taking 10 measurements for each container in order to ensure the accuracy of our results. Meanwhile, the "ASD field spectroradiometer" was warmed up for more than half an hour before measuring the canopy spectral reflectance. The instrument was recalibrated by "whiteboard" for each measurement of one group.

Due to the influence of the instrument itself, the measured canopy spectral reflectance data are relatively noisy in the ranges of 325-400 nm and 1000-1075 nm. In this study, we used RS^3 spectrum analysis software equipped for ASD to perform low-pass filtering on the canopy measurement spectral curve. To preserve the original spectral characteristics of the features, the spectral curve burrs caused by instrument noise were removed, and the range of 400-900 nm was selected for canopy spectral analysis.

a) Model simulated data

The PROSAIL model, combining the PROSPECT leaf optical properties model and the SAIL canopy bidirectional reflectance model, has been widely used to study plant canopy spectral and directional reflectance in the solar domain [47-49]. The PROSAIL model simulates the reflectance and transmittance spectra of broad vegetation canopy level from 400 nm to 2500 nm at a 1 nm interval.

In our study, the PROSAIL model was used for simulating canopy reflectance by different defined ratios. The input variables of PROSAIL were set according to the measured biochemical contents and auxiliary

parameters in the field. Focusing on the fresh leaves, the brown pigment content (C_{brown}) was neglected with 0.0 ug.cm^{-2} [50]. The leaf mesophyll structure (N) was not measurable, therefore we used an artificial setting from 1.0 to 4.0, which was consistent with previous research [51]. The value range of each input parameter was listed in Table 1. We used uniform distribution as the probability density function and generated 500 input parameter sets using Monte Carlo method. Among them, 100 groups were generated without considering interspecies competition, and 100 groups were set for different mixture ratio.

Before simulating the data with the PROSAIL model, the simulated canopy spectrum and the measured canopy spectrum were compared. The results showed that when the mesophyll structural parameter was adjusted appropriately, the difference between the measured canopy spectrum and the PROSAIL simulated spectrum did not exceed 3% in the visible band of 400-700 nm. In the near-infrared band, compared with visible light, a large error (with a maximum of approximately 10%) was noted. However, this model was still selected for our research mainly because it can simulate canopy reflectance in various gradient contents and the simulated spectrum is consistent with the measured spectrum in the change trend, which guarantees we can focus on the spectrum differences caused by the interspecies mixture ratio. In addition, the error between the simulated and measured spectrums was the smallest at the red edge. This corresponds to the selection of the sensitive spectral index as most of sensitive bands are selected according to their position at the red edge, which consequently reduces the influence of the systematic error.

In general, we used the PROSAIL model to simulate the canopy spectral reflectance in different mixture ratio based on the measured biochemical composition data and auxiliary data. An error analysis showed that the simulated dataset can be used as supplementary data for estimating the *CCC* as there exists great consistency between these two data resources.

b) Canopy spectral analysis of *S. alterniflora* and *P. australis*

Based on the measured data at different phases in the field, the changes in canopy spectra of pure *S. alterniflora* and pure *P. australis* for different months were compared and analyzed.

As shown in the Fig. 2a), the canopy spectral characteristics of *S. alterniflora* change significantly over time. The plants entered the germination period in April and then entered the growth phase, which caused the near-infrared reflectance of the canopy spectrum to increase significantly. Then, by July, the near-infrared reflectance reached the highest value, and after, the spectral reflectance gradually decreased, reaching the lowest value in November, indicating that the canopy spectrum is significantly affected by the soil background during this period.

Table 1. Setting model parameters for PROSAIL.

a) Without distinguishing interspecies competition (100 simulated datasets)			
Model parameters	Unit	Range	Mean
Leaf mesophyll structure (N)	--	1.0–4.0	2.58
chlorophyll (Cab)	ug·cm^{-2}	10.0–80.0	47.13
carotenoid (Car)	ug·cm^{-2}	1.0–15.0	7.61
Leaf water content (Cw)	g·cm^{-2}	0.007–0.060	0.034
Dry matters (Cm)	g·cm^{-2}	0.002–0.020	0.011
Leaf area index (LAI)	--	2.0–5.5	3.73
Average leaf angle (ALA)	°	40.0–65.0	53.64

b) Considering interspecies competition (100 sets for each competition ratio)				
Model parameters	Unit	Ratios	Range	Mean
Leaf mesophyll structure (N)	--	Pure S.	1.0–4.0	2.55
		S:P = 3:1	1.0–4.0	2.58
		S:P = 1:1	1.0–4.0	2.36
		S:P = 1:3	1.0–4.0	2.52
chlorophyll (Cab)	*ug·cm^{-2}*	Pure S.	10.0–60.0	33.37
		S:P = 3:1	25.0–80.0	50.71
		S:P = 1:1	20.0–80.0	45.86
		S:P = 1:3	15.0–75.0	41.06
carotenoid (Car)	*ug·cm^{-2}*	Pure S.	1.0–10.0	5.67
		S:P = 3:1	2.0–10.0	6.04
		S:P = 1:1	2.5–15.0	8.90
		S:P = 1:3	2.5–15.0	8.77
Leaf water content (Cw)	*g·cm^{-2}*	Pure S.	0.010–0.060	0.035
		S:P = 3:1	0.010–0.050	0.029
		S:P = 1:1	0.008–0.060	0.035
		S:P = 1:3	0.007–0.060	0.035
Dry matter (Cm)	*g·cm^{-2}*	Pure S.	0.003–0.020	0.011
		S:P = 3:1	0.004–0.020	0.012
		S:P = 1:1	0.003–0.020	0.012
		S:P = 1:3	0.002–0.020	0.011
Leaf area index (LAI)		Pure S.	3.0–5.0	3.97
		S:P = 3:1	3.4–5.5	4.49
		S:P = 1:1	2.0–4.8	3.51
		S:P = 1:3	2.4–4.4	3.49
Average leaf angle (ALA)	°	Pure S.	50–65	54.56
		S:P = 3:1	40–60	50.02
		S:P = 1:1	45–65	55.58
		S:P = 1:3	40–65	53.21

Similarly, the canopy spectral reflectance of *P. australis* also varied significantly (Fig. 2b). Note that the canopy spectrum reflectance difference between *S. alterniflora* and *P. australis* was the most significant, including that in the visible band and the near-infrared band in April, corresponding to the different phenological periods of these two species. As the growth period progresses, until July, the spectral difference between *S. alterniflora* and *P. australis* in the visible band is very small and the reflectance of *S. alterniflora* exceeds that of *P. australis* in the near-infrared band (Fig. 3b). Similarly, *P. australis* entered a withering period in November and the difference in reflectance between the two species in the near-infrared band increased again, showing that both species were clearly affected by the underlying surface (Fig. 3c).

The canopy spectrum analysis over different months shows that it is necessary to select a suitable period to properly estimate the *CCC*. We conducted research on the changes of canopy spectra at different time-phase typical bands in different interspecies competitions. As shown in Fig. 4, interspecies competition plays a significant role on the canopy spectral reflectance, with different growth periods showing different degrees of changes.

In April, the canopy spectrum is quite different under the different mixture ratio at the blue and green bands (Figs 4a,b), mainly owing to the different phenological periods of *S. alterniflora* and *P. australis.* For May and June, both *S. alterniflora* and *P. australis* entered the rapid growth period, and the spectrum difference was weakened in the red band and increased in the infrared band (Figs 4c,d). Also, note that the bands were affected to different degrees based on species competition. In July, the overall trend of the canopy spectrum in the typical bands was similar to that of pure *S. alterniflora*, while the extent caused by competition was different (Figs. 4a,d). We can see that the phenological period of the species was

affected due to the interspecies competition, which was seen in the rebound of reflectance of the canopy spectrum. Furthermore, interspecies competition played a dominant role in the spectrum of the mixed canopy when *S. alterniflora* was dominant, resulting in a very small difference with canopy spectrum of pure *S. alterniflora.*

Overall, interspecies competition caused a serious impact on the canopy spectral reflectance, lasting from germination to the period of decline. We also found that competition performed an obvious impact of species original growth cycle, which is reflected in the canopy spectrum. These results provide a basis for follow-up research regarding *CCC* estimation. The canopy spectral reflectance of the two species in different months at different competition levels were measured in order to determine a suitable period for *CCC* estimation (Fig. 5).

From Fig. 5, we can determine that the canopy spectrums of *S. alterniflora* and *P. australis* have excellent discrimination in April and November due to the difference in phenological period. It should be noted that this is not as defined in other months. However, the vegetation reduced substantially in November and the canopy spectrum was greatly affected by soil background, which was not suitable for inversion of *CCC*.

c) Single index selection of *CCC* without considering competition.

Thus far, our research showed that it is beneficial to estimate *CCC* under the conditions of interspecies competition in April. Therefore, we combined the measured data and the PROSAIL model simulated data for the inversion of *CCC* at different levels of interspecies competition for April.

Herein, 46 different spectral indices were evaluated to estimate *CCC* (Appendix, 46 indices are represented by ordinal serial numbers). The canopy sensitive spectral index was screened based on the spectral index
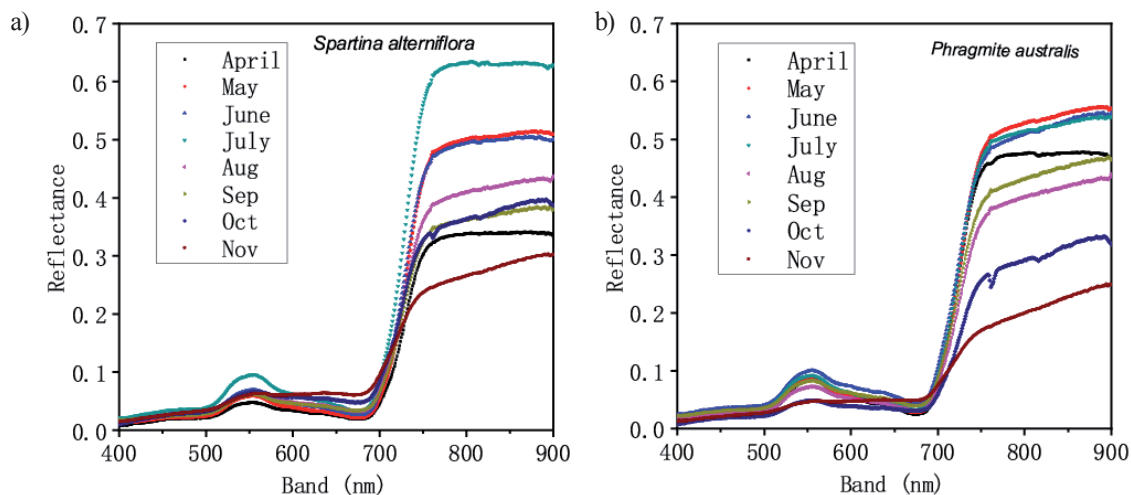

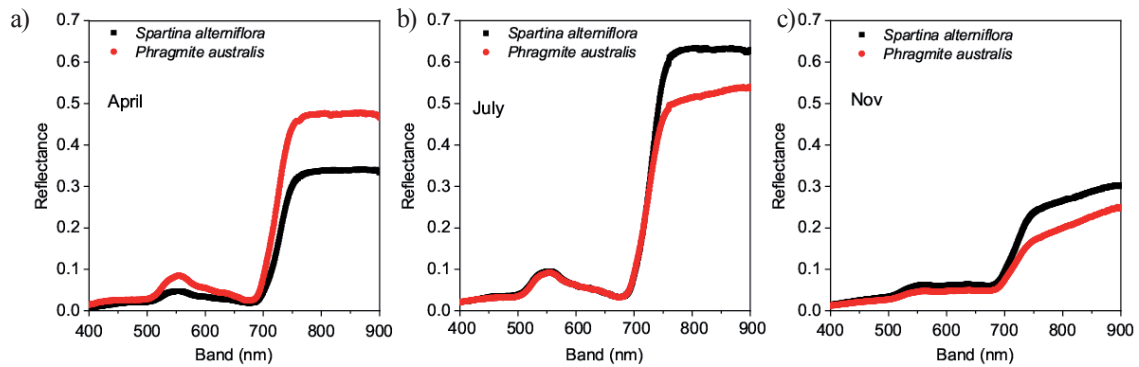Fig. 2 Average canopy reflectance of *S. alterniflora* a) and *P. australis* b) by different months

Fig. 3. Canopy reflectance of *S. alterniflora* and *P. australis* in a) April, b) July, and c) November.

library constructed using the 46 spectral indices without distinguishing the interspecies competition based on the PROSAIL model simulated dataset. We simulated 100 sets of biochemical composition data and spectral reflectance data to create basic datasets. Then, the correlation between different spectral indices (of the 46) and the simulated *CCC* were analyzed. Finally, without considering interspecies competition, we obtained V19 and V39 as the maximum positive correlation and minimum negative correlation indices, respectively. Fig. 6 shows the fitting line between the sensitive spectral index and *CCC*. It can clearly be seen that V19 and V39 are significantly correlated with *CCC*.

d) Single index selection of *CCC* considering competition.

The PROSAIL model was used to simulate canopy reflectance with specific model input parameters according to field measured data ranges of different mixture ratio. Then, the sensitive spectral index was screened from the 46 indices by determining interspecies competition. This screening method was similar to the maximum (or minimum) correlation analysis calculated previously. The statistical results of the sensitive spectral index at different ratios are summarized in Table 2.
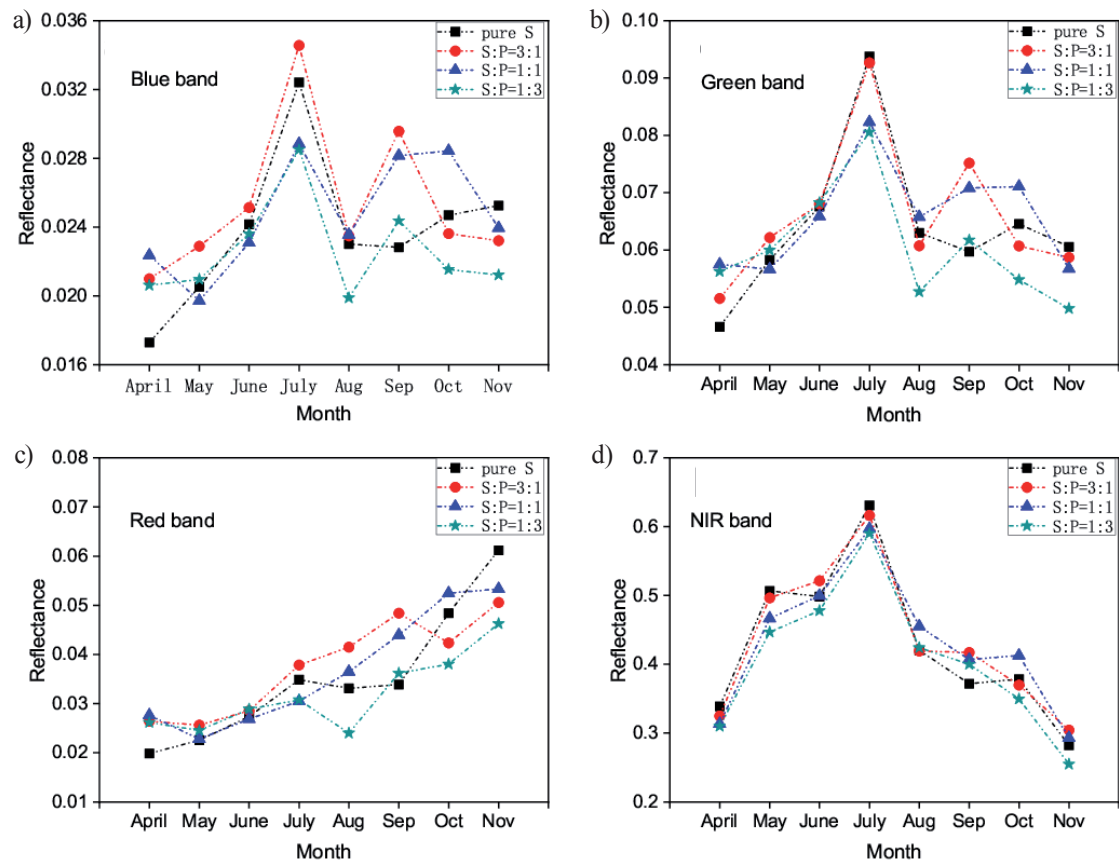

Fig. 4. Canopy reflectance changes in typical bands by months under different levels of interspecies competition.
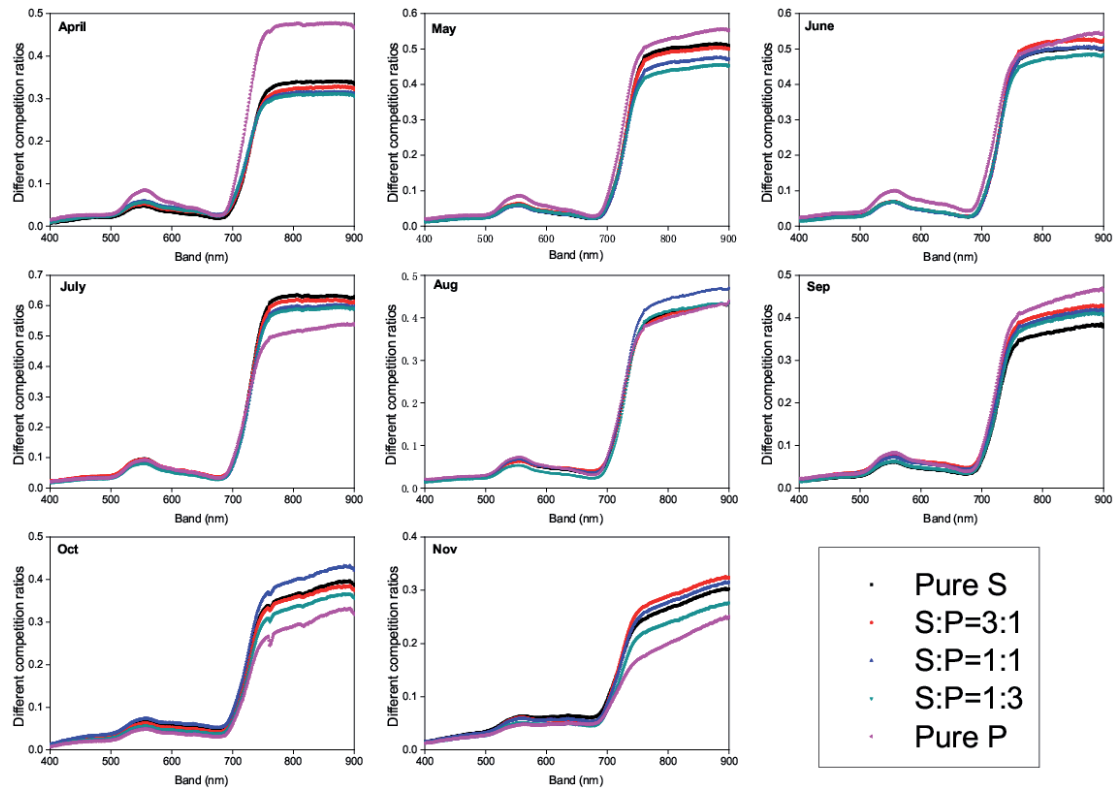
Fig. 5. Canopy spectrum changes at different interspecies competitions separated by months.

According to the statistical results listed in Table 2, the sensitive indices are different when considering interspecies competitions, indicating that the single sensitive index is unstable.

e) *CCC* estimation by multi-indices.

Based on the inversion of the *CCC* by single sensitive index, we focused on how to take advantage of the multi-sensitive indices when estimating of *CCC*. Therefore, we chose to integrate multiple spectral indices to build a multi-index collaborative model via a back propagation (BP) neural network for the inversion of *CCC*. Further, the differences between multi-indices and single index models were compared. Moreover,

we evaluated whether to consider the interspecies competition also using multi-indices.

Neural networks are widely used in various fields because of their strong nonlinear mapping and self-learning capability [37, 42, 52-56]. As an artificial intelligence method, a neural network model can identify the complicated linear and nonlinear relationships that exist between chlorophyll content and sensitive indices [10, 37, 57]. Note that neural network model structures are much more complicated than single index regression models. In our study, a typical scaled conjugate gradient BP algorithm used in learning algorithms was selected. During the BP training process, one hidden layer and
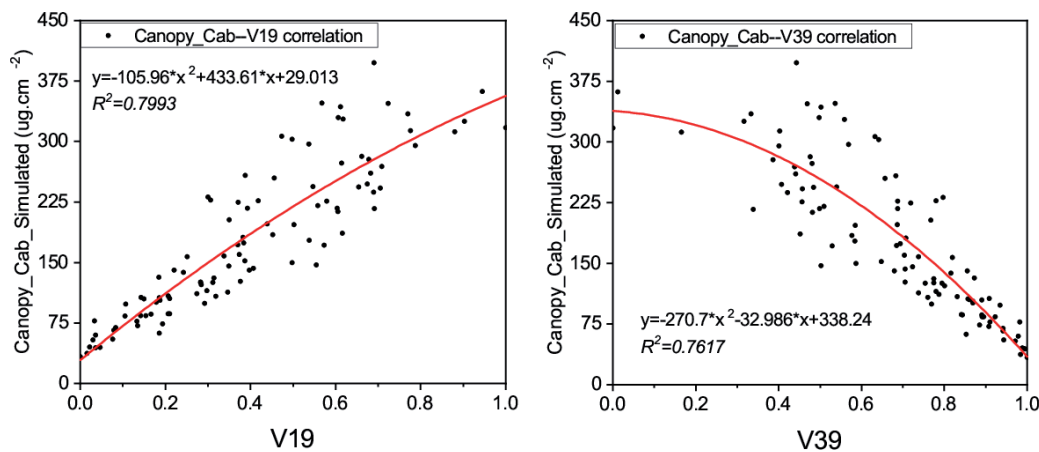

Fig. 6. Relationship between the sensitive spectral index and *CCC* without distinguishing interspecies competition.

Table 2 Sensitive spectral indices under different canopy interspecies competition.

Ratio	Sensitive indices
Pure S	V22, V39
S:P = 3:1	V19, V27
S:P = 1:1	V19, V39
S:P = 1:3	V46, V27

two hidden layers were both applied to estimate *CCC*. Therefore, the topological structure of the BP neural network contained five selected sensitive indices as factors in the input layer, one or two hidden layers and one output neuron for *CCC*. Herein, the input variables for this model were the V22, V19, V39, V46, and V27 indices chosen for their different mixture ratio (Table 2). The number of neurons were setting according to the former research.

Results and Discussion

The Single Index Inversion of Chlorophyll Content without Considering Competition

Note that our single index model was verified using the field measured data. As shown in Fig. 7, the correlation coefficient of R^2 reached 0.719 and 0.688 for V19 and V39, respectively, which were slightly lower than that of the model simulated data. Further, V19 and V39 revealed the limitation of the data as the estimated results were higher than the actual measured values, and the degree of overestimation increased with the increasing tendency of *CCC*.

The Single Index Inversion of Chlorophyll Content Considering Competition

Similarly, the simulated data were used to fit the relationship between selected sensitive index in Table 2 and the *CCC*, as shown in Fig. 8.

The fitting precision of the sensitive spectral index and the *CCC* was higher than that without distinguishing competition, indicating that it is necessary for single sensitive index to distinguish interspecies competition when estimating *CCC*. Fig. 9 verifies these results using measured data, except in the case of pure *S. alterniflora* (Fig. 7). For the estimation of pure *S. alterniflora*, the accuracy was lower, even lower than the indiscriminate competition, compared with the other mixture ratio. We concluded that this is a result of the difference in the phenological growth periods between the *S. alterniflora* and *P. australis* in April, where *S. alterniflora* was in the early growth stage prior to *P. australis* and therefore, the measured canopy spectrum of pure *S. alterniflora* was susceptible to the background surface. Conversely, for the mixing ratios in the other experimental control boxes, well-grown *P. australis* helps to reduce the influence of the underlying surface, shrinking the error between the simulated and measured data.

The coefficient of determination (R^2) and the root mean square error (*RMSE*) for the estimating *CCC* by single sensitive spectral index are listed in Table 3. It is clear that a higher R^2 and a lower *RMSE* were obtained by distinguishing interspecies competition with the exception, again, of pure *S. alterniflora*. Although the estimation accuracy of R^2 for pure *S. alterniflora* was slightly lower than that of total samples, the *RMSE* obtained 60.21 ug.cm^{-2}, is better than 63.53 ug.cm^{-2}. Overall, it is necessary to premeditate the interspecies competition to adequately estimate the *CCC*.
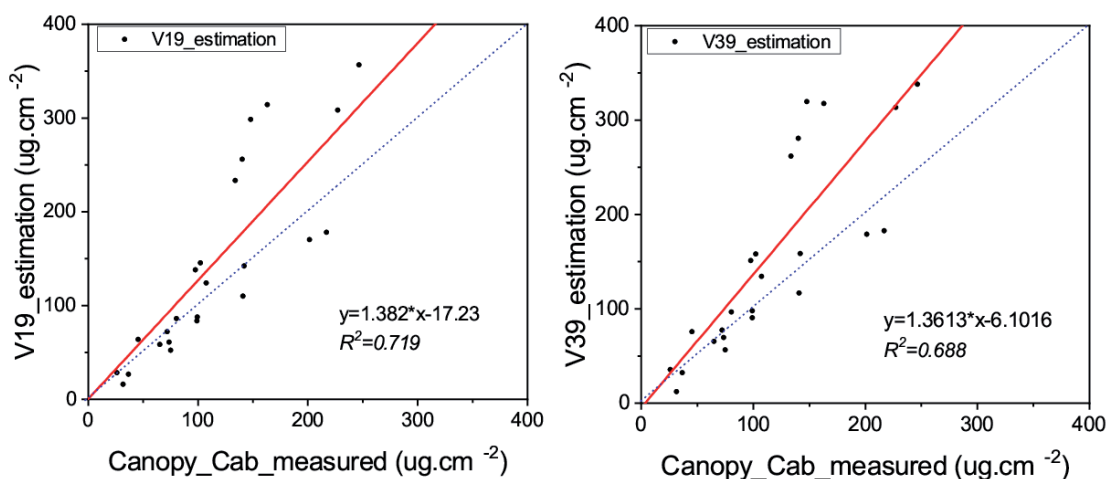

Fig. 7. Relationship between the predicted and measured values of the *CCC* without distinguishing interspecies competition.
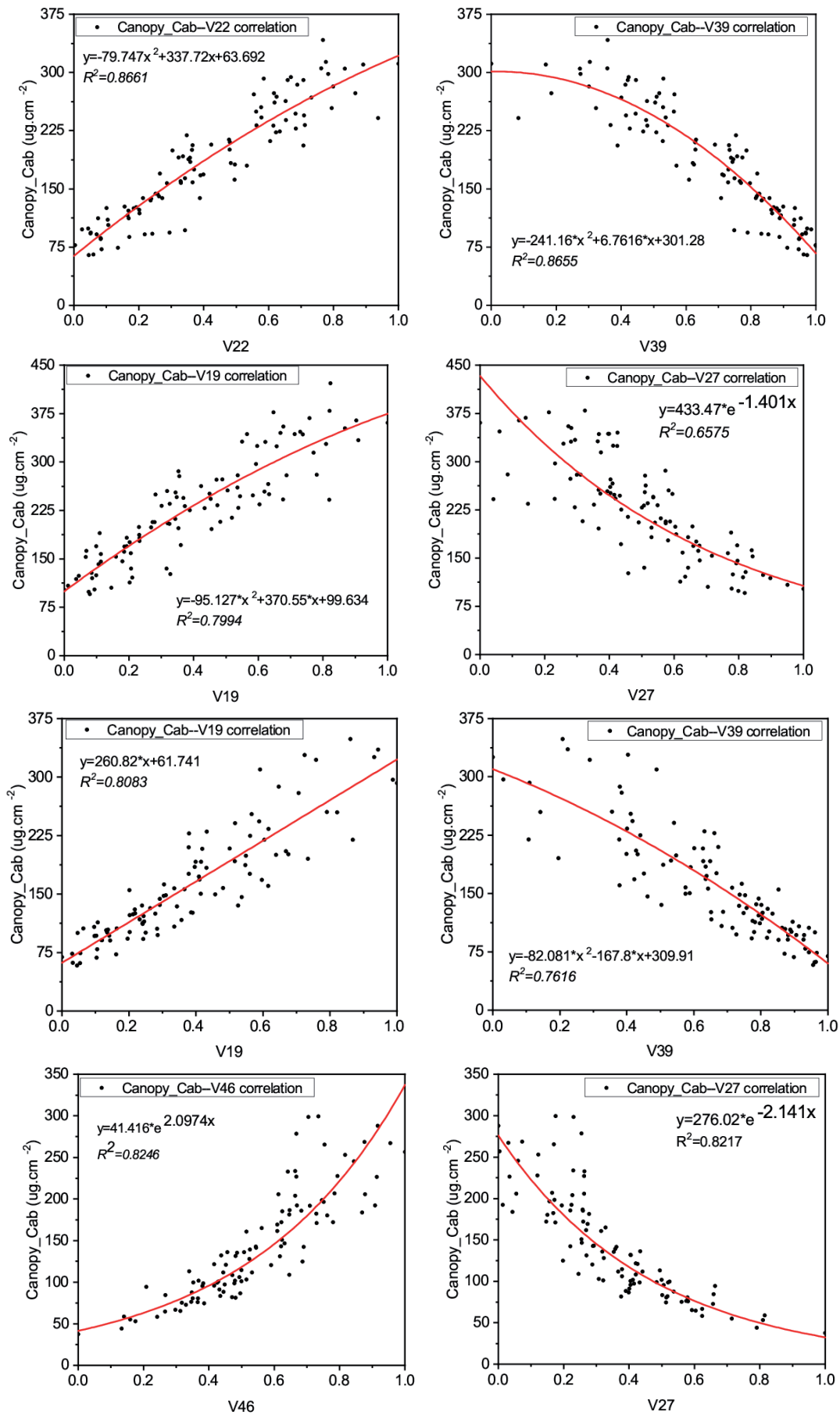
Fig. 8. Fitted relationship between sensitive spectral index and *CCC* under different interspecies competition based on model simulated data.

Table 3. Inversion of single spectral index for different mixture ratio and total samples.

Ratios	R^2	$RMSE$ (ug.cm^{-2})
Pure S	0.60	60.21
S:P = 3:1	0.4645	30.69
S:P = 1:1	0.8953	12.47
S:P = 1:3	0.8158	17.23
Total samples	0.7190	63.53

Table 4 Coefficient of determination (R^2) and root mean square error ($RMSE$) for predicted and measured values between single index and back propagation (BP) neural network model without distinguishing interspecies competition.

Method	R^2	$RMSE$ (ug.cm^{-2})
Single index (V19)	0.7190	63.53
BP neural network	0.7729	53.01

The Multi-Indices Inversion of *CCC* without Considering Interspecies Competition

The neural network prediction model was established using the different sensitive indices selected for different interspecies mixture ratio. Similarly, a training model established by the BP neural network was used to predict *CCC* in April without distinguishing interspecies competition. The prediction results were validated with measured data as shown in Fig. 10.

Basing on the prediction results of the BP neural network (Fig. 10), the correlation coefficient R^2 obtained was 0.7729 with an improved overestimation by single index. The R^2 and $RMSE$ were compared between the single index and BP neural network model under the condition of no interspecies competition distinction and the results are summarized in Table 4.

Combining the multi-indices via BP neural network obtained a higher R^2 at an increase of 7.5%, while the $RMSE$ decreased by 16.56% compared with single index prediction without distinguishing competition.

These results indicate that the BP neural network model can couple the advantages of different sensitive indices to perform a strong anti-competitive strategy for estimating the *CCC*. And the prediction error was clearly reduced, indicating that combining multi-indices for the inversion has better applicability than using a single index.

The Multi-Indices Inversion of *CCC* by Considering Interspecies Competition

Similarly, the BP neural network was used to predict the *CCC* considering the levels of interspecies competition. The predicted results of R^2 and $RMSE$ were obtained through the BP neural network after 50 averaged training processes. To visually compare the different estimation results between the BP neural network model and the single spectral index, we summarized the R^2 and $RMSE$ values in Table 5.

It can be found in Table 5 that the accuracy of R^2 was significantly improved by using multi-spectral indices integration via the BP neural network model when considering interspecies competition. The increased range of R^2 changed from 3.57% to 20.37% and the prediction error $RMSE$ was reduced at varying degrees (maximum reduction of 23.78%) under different mixture ratio.

Combining the results of Tables 3 and Table 5, the $RMSE$ was significantly higher for pure growth condition, regardless of methods. This is mainly due to the mutual growth of *S. alterniflora* at the initial growth stage, in which the canopy reflectance is greatly affected by the underlying surface background, showing the typical mixed spectral characteristics of vegetation and soil.

Generally, combining multi-indices to estimate *CCC* synergistically via a BP neural network model can obtain a lower $RMSE$, by approximately 16.56%, than that of single spectral index model under the condition of no distinguishing interspecies competition. When considering the level of interspecies competition, the highest decrease in the $RMSE$ values obtained was 23.78%, indicating that combining multi-indices for the inversion of *CCC* cooperatively through BP neural network model can achieve much higher accuracy.

Table 5 Evaluation results for predicted and measured values obtained by both the single index and BP neural network model under interspecies competition.

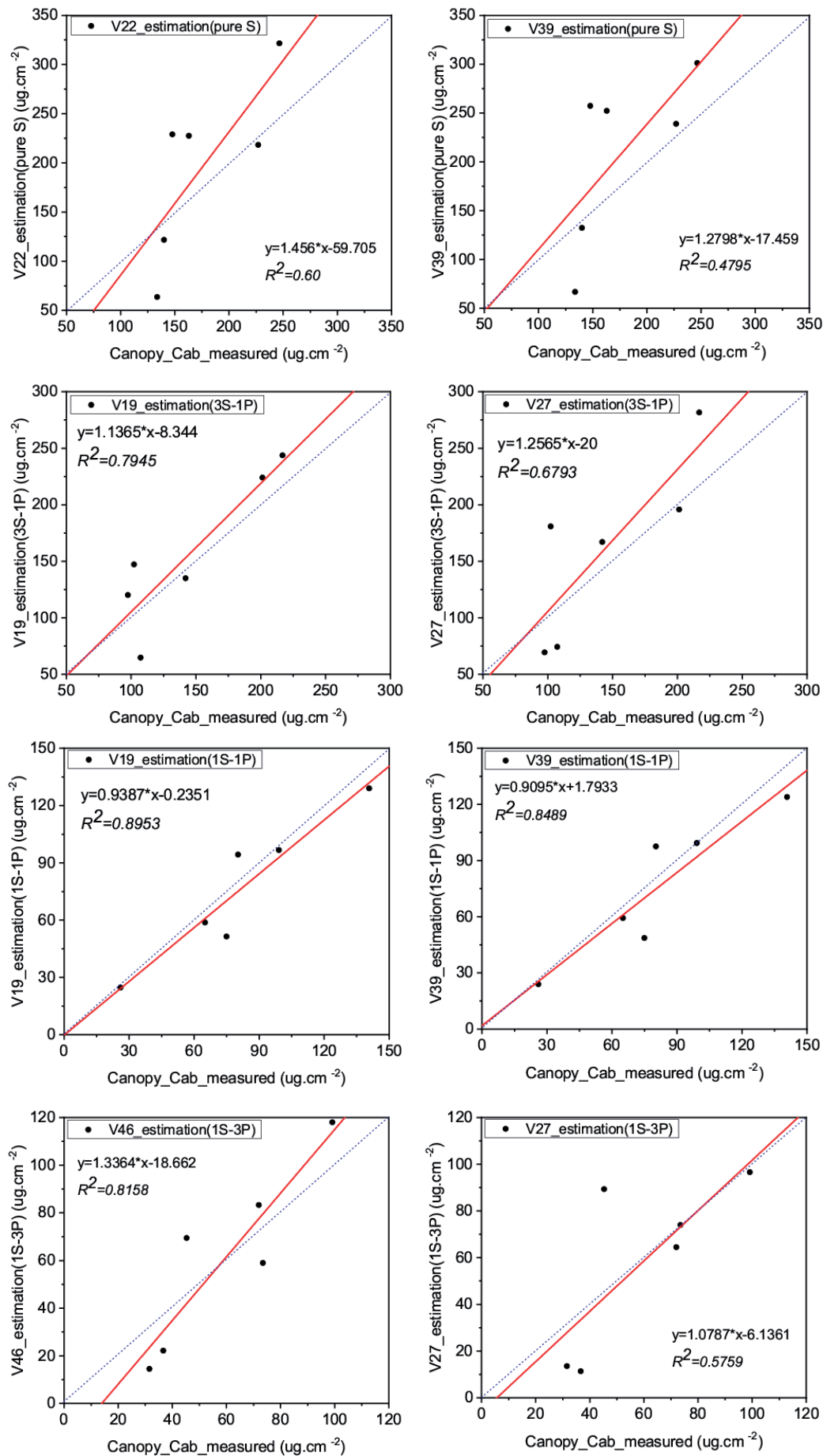| Competition ratio	R^2		$RMSE$ (ug.cm^{-2})	
	Single index	BP neural network	Single index	BP neural network
Pure S	0.60	0.7222	60.21	45.89
S:P = 3:1	0.4645	0.8532	30.69	26.62
S:P = 1:1	0.8953	0.9314	12.47	12.33
S:P = 1:3	0.8158	0.8449	17.23	13.58

Fig. 9. Fitting relationship between the predicted and measured values considering interspecies competition at the canopy scale.
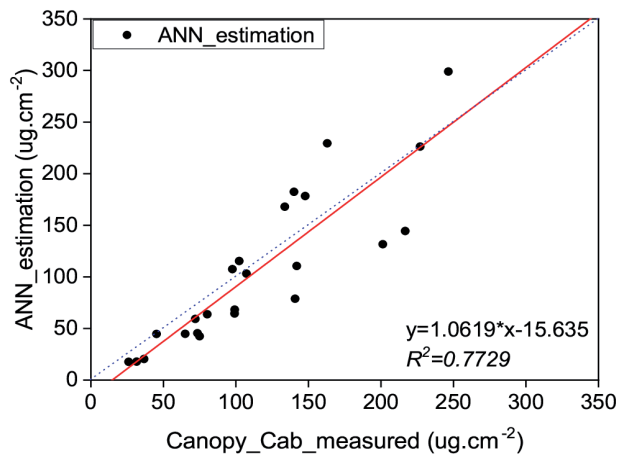
Fig. 10. Fitting relationship between the BP neural network model predicted values and measured values for *CCC* based on model simulated data.

In this study, we investigated *CCC* estimation of *S. alterniflora* and *P. australis* under different interspecies mixture ratio. The results indicate that the BP neural network model had a reliable ability to accurately estimate mixed *CCC*.

Owing to the influence of interspecies competition, it is insufficient to estimate *CCC* with a single spectral index. Beyond that, previous studies mainly focused on the mechanism and propagation between interspecies interaction among salt marsh vegetation [23, 58-62]. As clearly shown in Fig. 7, there exists a clear overestimation problem in estimating *CCC* using a single index. Thus, combining multi-indices via a BP neural network model was conducted. And the results showed that this overestimation could be significantly improved regardless of interspecies competition.

Multiple sensitive indices were integrated to alleviate the influence of mixture ratio. Interspecies competition, especially for the mixed canopy, influenced the BP neural network model, indicating that it may be best suited for specific datasets. In addition, both canopy chlorophyll content in chlorophyll a and b were estimated as they were measured separately. Finally, the same results were obtained by BP neural network model developed in our study. It is necessary to validate the model through checking the training degree to which the BP neural network model predicted *CCC* matches the measured data. Still, there remain several uncertain factors relating to model setup and its application capacity owing to the environmental variability and stochasticity in the growing stage of salt marsh vegetation [12]. Regardless, the model established herein provided a novel method or valuable insights to overcome or alleviate the influences of interspecies competition for the inversion of mixed *CCC*.

For the growth of *S. alterniflora* and *P. australis*, the level of nutrients, growth space, sunlight resource, and perhaps other unknown factors may affect the co-occurrence environment. The sensitive spectral indices

selected in this study (Appendix) showed that the bands were concentrated along the red edge and near-infrared regions, indicating that they are much more sensitive to *CCC* and have strong anti-interference abilities. We suggest that these sensitive bands have the potential of applying to build new vegetation indices for monitoring the region levels of invasive *S. alterniflora* using satellite or unmanned aerial vehicle (UAV) imaging for larger applications.

Conclusions

In this study, the canopy spectral reflectance was measured by different months at different interspecies mixture ratio between *S. alterniflora* and *P. australis* in a field control experiment. The typical canopy reflectance bands were analyzed by different ratios in each growing stage to evaluate the effect of interspecies competition. Based on the change of canopy reflectance, single sensitive index model and multi-indices combining via BP neural network model were established to estimate *CCC*. Both field measured dataset and model simulations were used. Furthermore, two situations were evaluated, one where interspecies competition was considered and one where it was not. Our results indicated that combining multi-indices through a BP neural network model by distinguishing mixture ratio can achieve satisfactory estimating results, as evaluated by the *R²* and *RMSE*.

The measured canopy spectral reflectance results indicated the conclusions that: (1) interspecies competition had a significant effect on the canopy reflectance at different growth periods. It's ideal to estimate *CCC* in mixed ratio from the end of April to the beginning of May owing to the largest canopy reflectance difference and (2) regarding the impact of estimating *CCC* by interspecies competition, our results show that considering the extent of interspecies competition can significantly improve the accuracy of the data. It can be inferred that the influence effected by interspecies competition will further affect the inversion of *CCC* and (3) the inversion accuracy was conspicuously better than the single sensitive spectral index compared with the multi-indices integration via BP neural network, as determined by the remarkably reduced *RMSE*. Further, it maintained a satisfied linear relationship between the predicted and measured values.

Therefore, it is crucial to consider interspecies competition by combining multi-indices to estimate chlorophyll content at the regional scale where the native and local species coexistence from remote sensing imagery.

Acknowledgements

Conflicts of Interest

The authors declare no conflicts of interest.

Appendix

The 46 spectral indices used in this study.

Num.	Index	Algorithm	Reference
V1	Normalized difference vegetation index(NDVI)	$\dfrac{R_{800} - R_{670}}{R_{800} + R_{670}}$	[63]
V2	Modified chlorophyll absorption ratio index(MCARI)	$\dfrac{[(R_{700} - R_{670}) - 0.2 * (R_{700} - R_{550})]}{(R_{700}/R_{670})}$	[64]
V3	Triangular vegetation index(TVI)	$0.5 * [120 * (R_{750} - R_{550}) - 200 * (R_{670} - R_{550})]$	[65]
V4	Modified chlorophyll absorption ratio index 1 (MCARI1)	$1.2 * [2.5 * (R_{800} - R_{670}) - 1.3 * (R_{800} - R_{550})]$	[66]
V5	Modified chlorophyll absorption ratio index 2 (MCARI2)	$\dfrac{1.5 * [2.5 * (R_{800} - R_{670}) - 1.3 * (R_{800} - R_{550})]}{\sqrt{(2 * R_{800} + 1)^2 - (6 * R_{800} - 5 * \sqrt{R_{670}}) - 0.5}}$	[66]
V6	Modified triangular vegetation index (MTVI2)	$\dfrac{1.5 * [1.2 * (R_{800} - R_{550}) - 2.5(R_{670} - R_{550})]}{\sqrt{(2 * R_{800} + 1)^2 - (6 * R_{800} - 5 * \sqrt{R_{670}} - 0.5)}}$	[66]
V7	Chlorophyll index	$\dfrac{R_{750}}{(R_{700} - R_{710}) - 1}$	[34]
V8	VI—700nm (VI$_{[700]}$)	$\dfrac{R_{700} - R_{670}}{R_{700} + R_{670}}$	[67]
V9	Chlorophyll Absorption Ratio Index (CARI)	$\dfrac{R_{700}}{R_{670}} * \dfrac{670 * a + R_{670} + b}{\sqrt{a^2 + 1}}$ $a = \dfrac{R_{700} - R_{550}}{150}; b = R_{550} - 550 * a$	[68]
V10	Enhanced Vegetation Index (EVI)	$2.5 * ((R_{800} - R_{670})/(R_{800} - (6 * R_{670}) - (7.5 * R_{475}) + 1))$	[69]
V11	MCARI/OSAVI	$MCARI = [(R_{700} - R_{670}) - 0.2 * (R_{700} - R_{550})] * \dfrac{R_{700}}{R_{670}}$ $OSAVI = (1 + 0.16) * \dfrac{(R_{800} - R_{670})}{(R_{800} + R_{670} + 0.16)}$	[64]
V12	MCARI2-Wu/OSAVI2-Wu	$MCARI2_{Wu} = ((R_{750} - R_{705}) - 0.2 * (R_{750} - R_{550})) * (R_{750}/R_{705})$ $OSAVI2_{Wu} = (1 + 0.16) * (R_{750} - R_{705})/(R_{750} + R_{705} + 0.16)$	[70]
V13	Renormalised Difference Vegetation Index (RDVI)	$(R_{800} - R_{670})/\sqrt{(R_{800} + R_{670})}$	[71]
V14	Spectral Polygon Vegetation Index (SPVI)	$0.4 * 3.7 * (R_{800} - R_{670}) - 1.2 * \sqrt{(R_{530} - R_{670})^2}$	[72]

V15	Transformed Chlorophyll Absorption Ratio Index (TCARI)	$3 * ((R_{700} - R_{670}) - 0.2 * (R_{700} - R_{550}) * (R_{700}/R_{670}))$	[73]
V16	Transformed Chlorophyll Absorption Ratio Index (TCARI2-Wu)	$3 * ((R_{750} - R_{705}) - 0.2 * (R_{750} - R_{550}) * (R_{750}/R_{705}))$	[70]
V17	TCARI/OSAVI	$TCARI = 3 * ((R_{700} - R_{670}) - 0.2 * (R_{700} - R_{550}) * (R_{700}/R_{670}))$ $OSAVI = (1 + 0.16) * (R_{800} - R_{670})/(R_{800} + R_{670} + 0.16)$	[73]
V18	TCARI2-Wu/OSAVI2-Wu	$TCARI2_{Wu} = 3 * ((R_{750} - R_{705}) - 0.2 * (R_{750} - R_{550}) * (R_{750}/R_{705}))$ $OSAVI2_{Wu} = (1 + 0.16) * (R_{750} - R_{705})/(R_{750} + R_{705} + 0.16)$	[70]
V19	Modified NDVI (MNDVI1)	$(R_{755} - R_{745})/(R_{755} + R_{745})$	[74]
V20	Double Difference Index (DD)	$(R_{749} - R_{720}) - (R_{701} - R_{672})$	[75]
V21	New Double Difference Index (DDn)	$2 * (R_{710} - R_{(710-50)} - R_{(710+50)})$	[76]
V22	Modified NDVI (MNDVI8)	$(R_{755} - R_{730})/(R_{755} + R_{730})$	[74]
V23	Derivative reflectance at D690 (D_red)	D_{690}	[77]
V24	Double Peak Index (DPI)	$(D_{688} * D_{710})/D_{697}{}^2$	[78]
V25	Modified NDVI (mNDVI)	$(R_{800} - R_{680})/(R_{800} + R_{680} - 2R_{445})$	[79]
V26	Modified NDVI (mND705)	$(R_{750} - R_{705})/(R_{750} + R_{705} - 2R_{445})$	[79]
V27	D2--Canopy scale	$\dfrac{D_{705}}{D_{722}}$	[78]
V28	Improved Soil Adjusted Vegetation Index (MSAVI)	$0.5 * \left(2 * R_{800} + 1 - \sqrt{(2 * R_{800} + 1)^2 - 8 * (R_{800} - R_{670})}\right)$	[80]
V29	D1--Canopy scale, related to Chlorophyll fluorescence	$\dfrac{D_{730}}{D_{706}}$	[78]
V30	mSR2--Canopy scale, related to Chlorophyll and LAI	$\left(\dfrac{R_{750}}{R_{705}}\right) - \dfrac{1}{\sqrt{\left(\left(\dfrac{R_{750}}{R_{705}}\right) + 1\right)}}$	[81]
V31	MERIS Terrestrial chlorophyll index (MTCI)	$\dfrac{R_{754} - R_{709}}{R_{709} - R_{681}}$	[82]
V32	Red-edge position linear interpolation (REP_Li)	$700 + 40 * ((R_{670} + R_{780}/2)/(R_{740} - R_{700}))$	[83]
V33	Normalized Pigment chlorophyll index (NPCI)	$\dfrac{R_{680} - R_{430}}{R_{680} + R_{430}}$	[84]
V34	Green NDVI --Canopy scale, related to Chlorophyll-a	$\dfrac{R_{800} - R_{550}}{R_{800} + R_{550}}$	[85]
V35	Structure Insensitive Pigment Index (SIPI)	$\dfrac{R_{800} - R_{445}}{R_{800} - R_{680}}$	[84]
V36	Simple Ratio Pigment Index (SRPI)	$\dfrac{R_{430}}{R_{680}}$	[84]
V37	Vogelmann ---leaf scale, related to Chlorophyll	$\dfrac{R_{740}}{R_{720}}$	[86]
V38	Vogelmann3---leaf scale, related to Chlorophyll	$\dfrac{D_{715}}{D_{705}}$	[86]

V39	Vogelmann2---leaf scale, related to Chlorophyll	$\dfrac{R_{734} - R_{747}}{R_{715} + R_{726}}$	[86]
V40	Curvature Index (CI)	$R_{675} * R_{690}/R_{683}{}^2$	[78]
V41	Modified simple ratio	$(R_{800} - R_{445})/(R_{680} - R_{445})$	[79]
V42	mSR_705	$(R_{750} - R_{445})/(R_{705} - R_{445})$	[79]
V43	Pigment specific simple ratio Chlorophyll	$\dfrac{R_{800}}{R_{680}} + \dfrac{R_{800}}{R_{635}}$	[87]
V44	Reflectance at the inflection point	$(R_{670} + R_{780})/2$	[83]
V45	Gitelson ratio green	$\dfrac{R_{800}}{R_{550}} - 1$	[88]
V46	Red edge inflection point	$\dfrac{700 + 40 * \left(\left(\dfrac{R_{670} + R_{780}}{2} - R_{700}\right)/(R_{740} - R_{700})\right)}{100}$	[83]

References

1. GABLER C.A., OSLAND M.J., GRACE J.B., STAGG C.L., DAY R.H., HARTLEY S.B., MCLEOD J.L. Macroclimatic change expected to transform coastal wetland ecosystems this century. *Nature Climate Change*, **7** (2), 142, **2017**.

2. HE Q., LI H., XU C., SUN Q., BERTNESS M.D., FANG C., SILLIMAN B.R. Consumer regulation of the carbon cycle in coastal wetland ecosystems: Consumer regulation of the carbon cycle. Philosophical Transactions of the Royal Society B: Biological Sciences, **375** (1814), **2020**.

3. KELLEWAY J.J., CAVANAUGH K., ROGERS K., FELLER I.C., ENS E., DOUGHTY C., SAINTILAN N. Review of the ecosystem service implications of mangrove encroachment into salt marshes. Global Change Biology, **23** (10), 3967, **2017**.

4. FENG J., ZHOU J., WANG L., CUI X., NING C., WU H., LIN G. Effects of short-term invasion of Spartina alterniflora and the subsequent restoration of native mangroves on the soil organic carbon, nitrogen and phosphorus stock. Chemosphere, **184**, 774, **2017**.

5. ZANG Z., ZOU X., ZUO P., SONG Q., WANG C., WANG J. Impact of landscape patterns on ecological vulnerability and ecosystem service values: An empirical analysis of Yancheng Nature Reserve in China. Ecological Indicators, **72**, 142, **2017**.

6. CHENG L., ZHANG Y., SUN H. Vegetation Cover Change and Relative Contributions of Associated Driving Factors in the Ecological Conservation and Development Zone of Beijing , China, **29** (1), 53, **2020**.

7. BERNAL B., MEGONIGAL J.P., MOZDZER T.J. An invasive wetland grass primes deep soil carbon pools. Global Change Biology, **23** (5), 2104, **2017**.

8. LONG A.L., KETTENRING K.M., HAWKINS C.P., NEALE C.M.U. Distribution and Drivers of a Widespread, Invasive Wetland Grass, Phragmites australis, in Wetlands of the Great Salt Lake, Utah, USA. Wetlands, **37** (1), 45, **2017**.

9. GAO G.-F., LI P.-F., ZHONG J.-X., SHEN Z.-J., CHEN,J., LI Y.-T., ZHENG H.-L. Spartina alterniflora invasion alters soil bacterial communities and enhances soil N_2O emissions by stimulating soil denitrification in mangrove wetland. Science of The Total Environment, **653**, 231, **2019**.

10. LIU P., SHI R., ZHANG C., ZENG Y., WANG J., TAO Z., GAO W. Integrating multiple vegetation indices via an artificial neural network model for estimating the leaf chlorophyll content of Spartina alterniflora under interspecies competition. Environmental Monitoring and Assessment, **189** (11), **2017**.

11. ZHENG Y., BU N.-S., LONG X.-E., SUN J., HE C.-Q., LIU X.-Y., CHEN X.-P. Sulfate reducer and sulfur oxidizer respond differentially to the invasion of Spartina alterniflora in estuarine salt marsh of China. Ecological Engineering, **99**, 182, **2017**.

12. GE Z., CAO H., ZHANG L. A process-based grid model for the simulation of range expansion of Spartina alterniflora on the coastal saltmarshes in the Yangtze Estuary. Ecological Engineering (Vol. **58**). Elsevier B.V, **2013**.

13. LIU J., HAN, R.-M., SU H.-R., WU Y.-P., ZHANG L.-M., RICHARDSON C.J., WANG G.-X. Effects of exotic Spartina alterniflora on vertical soil organic carbon distribution and storage amount in coastal salt marshes in Jiangsu, China. Ecological Engineering, **106**, 132, **2017**.

14. GE Z., GUO H., ZHAO B., ZHANG L. Journal of Geophysical Research Biogeosciences. Journal of Geophysical Research: Biogeosciences, **119**, 1129, **2014**.

15. HU Z.J., GE Z.M., MA Q., ZHANG Z.T., TANG C.D., CAO H., BIN, ZHANG L.Q. Revegetation of a native species in a newly formed tidal marsh under varying hydrological conditions and planting densities in the Yangtze Estuary. Ecological Engineering, **83**, 354, **2015**.

16. CUI J., CHEN X., NIE M., FANG S., TANG B., QUAN Z., FANG C. Effects of Spartina alterniflora Invasion on the Abundance, Diversity, and Community Structure of Sulfate Reducing Bacteria along a Successional Gradient of Coastal Salt Marshes in China. Wetlands, **37** (2), 221, **2017**.

17. YANG W., JEELANI N., ZHU Z., LUO Y., CHENG X., AN S. Alterations in soil bacterial community in relation to Spartina alterniflora Loisel. invasion chronosequence in the eastern Chinese coastal wetlands. Applied Soil Ecology, **135**, 38, **2019**.

18. ROOSJEN P.P.J., BREDE B., SUOMALAINEN J.M., BARTHOLOMEUS H.M., KOOISTRA L., CLEVERS J.G.P.W. Improved estimation of leaf area index and leaf chlorophyll content of a potato crop using multi-angle spectral data – potential of unmanned aerial vehicle imagery. International Journal of Applied Earth Observation and Geoinformation, **66**, 14, **2018**.

19. DZIWULSKA-HUNEK A., ĆWINTAL M., NIEMCZYNOWICZ A., BOROŃ B., MATWIJCZUK A. Effect of stress caused by electromagnetic stimulation on the fluorescence lifetime of chlorophylls in alfalfa leaves. Polish Journal of Environmental Studies, **28** (5), 3133, **2019**.

20. NGUY-ROBERTSON A.L., ARKEBAUER T.J., PENG Y., NGUY-ROBERTSON A., ARKEBAUER T., GITELSON A.A. Assessment of Canopy Chlorophyll Content Retrieval in Maize and Soybean: Implications of Hysteresis on the Development of Assessment of Canopy Chlorophyll Content Retrieval in Maize and Soybean: Implications of Hysteresis on the Development of Generic A, **2017**.

21. OU Z., CAO J., SHEN W., TAN Y., HE Q., PENG Y. Understory Flora in Relation to Canopy Structure, Soil Nutrients, and Gap Light Regime: a Case Study in Southern China. Polish Journal of Environmental Studies, **24** (6), 2559, **2015**.

22. CLEVERS J.G.P.W., GITELSON A.A. Remote estimation of crop and grass chlorophyll and nitrogen content using red-edge bands on sentinel-2 and-3. International Journal of Applied Earth Observation and Geoinformation, **23** (1), 344, **2013**.

23. YUAN Y., ZHANG C., LI D. The Effect of Artificial Mowing on the Competition of Phragmites australis and Spartina alterniflora in the Yangtze Estuary. Scientifica, **2017**, **2017**.

24. YANG H., YANG X., ZHANG Y., HESKEL M.A., LU, X., MUNGER J.W., TANG J. Chlorophyll fluorescence tracks seasonal variations of photosynthesis from leaf to canopy in a temperate forest. Global Change Biology, **23** (7), 2874, **2017**.

25. DELEGIDO J., VAN WITTENBERGHE S., VERRELST J., ORTIZ V., VEROUSTRAETE F., VALCKE R., MORENO J. Chlorophyll content mapping of urban vegetation in the city of Valencia based on the hyperspectral NAOC index. Ecological Indicators, **40** (2014), 34, **2014**.

26. ZHAO, Y., YAN, C., LU, S., WANG, P., QIU, G. Y., & LI, R. Estimation of chlorophyll content in intertidal mangrove leaves with different thicknesses using hyperspectral data. Ecological Indicators, **106**, 105511, **2019**.

27. DELEGIDO J., VAN WITTENBERGHE S., VERRELST J., ORTIZ, V., VEROUSTRAETE F., VALCKE R., MORENO J. Chlorophyll content mapping of urban vegetation in the city of Valencia based on the hyperspectral NAOC index. Ecological Indicators, **40**, 34, **2014**.

28. LIU J., HAN J., CHEN X., SHI L., ZHANG L. Nondestructive detection of rape leaf chlorophyll level based on Vis-NIR spectroscopy. Spectrochimica Acta - Part A: Molecular and Biomolecular Spectroscopy, **222**, 117202, **2019**.

29. SMITH S.M., LEE K.D. The influence of prolonged flooding on the growth of Spartina alterniflora in Cape Cod (Massachusetts, USA). Aquatic Botany, **127**, 53, **2015**.

30. XUE J., SU B. Significant Remote Sensing Vegetation Indices: A Review of Developments and Applications. Journal of Sensors, **2017**, 1353691, **2017**.

31. KORHONEN L., HADI, PACKALEN P., RAUTIAINEN M. Comparison of Sentinel-2 and Landsat 8 in the estimation of boreal forest canopy cover and leaf area index. Remote Sensing of Environment, **195**, 259, **2017**.

32. POTGIETER A.B., GEORGE-JAEGGLI B., CHAPMAN S.C., LAWS K., CADAVID L.A.S., WIXTED J., HAMMER G.L. Multi-spectral imaging from an unmanned aerial vehicle enables the assessment of seasonal leaf area dynamics of sorghum breeding lines. Frontiers in Plant Science, **8** (September), **2017**.

33. MALENOVSKÝ Z., TURNBULL J.D., LUCIEER A., ROBINSON S.A. Antarctic moss stress assessment based on chlorophyll content and leaf density retrieved from imaging spectroscopy data. New Phytologist, **208** (2), 608, **2015**.

34. GITELSON A.A., VIÑA A., CIGANDA V., RUNDQUIST D.C., ARKEBAUER T.J. Remote estimation of canopy chlorophyll content in crops. Geophysical Research Letters, **32** (8), 1, **2005**.

35. ZARCO-TEJADA P.J., BERJÓN A., LÓPEZ-LOZANO R., MILLER J.R., MARTÍN P., CACHORRO V., DE FRUTOS A. Assessing vineyard condition with hyperspectral indices: Leaf and canopy reflectance simulation in a row-structured discontinuous canopy. Remote Sensing of Environment, **99** (3), 271, **2005**.

36. VERRELST J., RIVERA J.P., LEONENKO G., ALONSO L., MORENO J. Optimizing LUT-based RTM inversion for semiautomatic mapping of crop biophysical parameters from sentinel-2 and -3 data: Role of cost functions. IEEE Transactions on Geoscience and Remote Sensing, **52** (1), 257, **2014**.

37. JAY S., GORRETTA N., MOREL J., MAUPAS F., BENDOULA R., RABATEL G., BARET F. Estimating leaf chlorophyll content in sugar beet canopies using millimeter- to centimeter-scale reflectance imagery. Remote Sensing of Environment, **198**, 173, **2017**.

38. JAY S., MAUPAS F., BENDOULA R., GORRETTA N. Retrieving LAI, chlorophyll and nitrogen contents in sugar beet crops from multi-angular optical remote sensing: Comparison of vegetation indices and PROSAIL inversion for field phenotyping. Field Crops Research, **210**, 33, **2017**.

39. LIU P., SHI R., GAO W. Estimating leaf chlorophyll contents by combining multiple spectral indices with an artificial neural network. Earth Science Informatics, **11** (1), **2018**.

40. DARVISHZADEH R., ATZBERGER C., SKIDMORE A., SCHLERF M. Mapping grassland leaf area index with airborne hyperspectral imagery: A comparison study of statistical approaches and inversion of radiative transfer models. ISPRS Journal of Photogrammetry and Remote Sensing, **66** (6), 894, **2011**.

41. LOCHERER M., HANK T., DANNER M., MAUSER W. Retrieval of seasonal leaf area index from simulated EnMAP data through optimized LUT-based inversion of the PROSAIL model. Remote Sensing, **7** (8), 10321, **2015**.

42. LIANG L., DI L., ZHANG L., DENG M., QIN Z., ZHAO S., LIN H. Estimation of crop LAI using hyperspectral vegetation indices and a hybrid inversion method. Remote Sensing of Environment, **165**, 123, **2015**.

43. VOHLAND M., MADER S., DORIGO W. Applying different inversion techniques to retrieve stand variables of summer barley with PROSPECT+SAIL. International Journal of Applied Earth Observation and Geoinformation, **12** (2), 71, **2010**.

44. YAO Y., LIU Q., LIU Q., LI X. LAI retrieval and uncertainty evaluations for typical row-planted crops at

different growth stages. Remote Sensing of Environment, **112** (1), 94, **2008**.

45. TANG L. Control of Spartina alterniflora by an integrated approach of clipping, waterlogging and ecological replacement with reed: an experimental study of ecological mechanisms. Ph.D. Dissertation: Fudan university, **2008**.

46. TANG L., GAO Y., LI B., WANG Q., WANG C.H., ZHAO B. Spartina alterniflora with high tolerance to salt stress changes vegetation pattern by outcompeting native species. Ecosphere, **5** (9), 1, **2014**.

47. JACQUEMOUD S., VERHOEF W., BARET F., BACOUR C., ZARCO-TEJADA P.J., ASNER G.P., USTIN S.L. PROSPECT + SAIL models: A review of use for vegetation characterization. Remote Sensing of Environment, **113** (SUPPL. 1), S56, **2009**.

48. BERGER K., ATZBERGER C., DANNER M., D'URSO G., MAUSER W., VUOLO F., HANK T. Evaluation of the PROSAIL model capabilities for future hyperspectral model environments: A review study. Remote Sensing, **10** (**1**), **2018**.

49. Retrieval of Biophysical Crop Variables from Multi-Angular Canopy Spectroscopy. Remote Sensing, **9** (7), 726, **2017**.

50. HOUBORG R., ANDERSON M., DAUGHTRY C. Utility of an image-based canopy reflectance modeling tool for remote estimation of LAI and leaf chlorophyll content at the field scale. Remote Sensing of Environment, **113** (1), 259, **2009**.

51. CECCATO P., FLASSE S., TARANTOLA S., JACQUEMOUD S., GRÉGOIRE J.-M. Detecting vegetation leaf water content using reflectance in the optical domain. Remote Sensing of Environment, **77** (1), 22, **2001**.

52. CHEN B., WU Z., WANG J., DONG J., GUAN L., CHEN J., XIE G. Spatio-temporal prediction of leaf area index of rubber plantation using HJ-1A/1B CCD images and recurrent neural network. ISPRS Journal of Photogrammetry and Remote Sensing, **102**, 148, **2015**.

53. CHEN J., QUAN W., CUI T., SONG Q. Estimation of total suspended matter concentration from MODIS data using a neural network model in the China eastern coastal zone. Estuarine, Coastal and Shelf Science, **155**, 104, **2015**.

54. JIA F., LIU G., LIU D., ZHANG Y., FAN W., XING X. Comparison of different methods for estimating nitrogen concentration in flue-cured tobacco leaves based on hyperspectral reflectance. Field Crops Research, **150**, 108, **2013**.

55. KALACSKA M., LALONDE M., MOORE T.R. Estimation of foliar chlorophyll and nitrogen content in an ombrotrophic bog from hyperspectral data: Scaling from leaf to image. Remote Sensing of Environment, **169**, 270, **2015**.

56. PÔÇAS I., GONÇALVES J., COSTA P.M., GONÇALVES I., PEREIRA L.S., CUNHA M. Hyperspectral-based predictive modelling of grapevine water status in the Portuguese Douro wine region. International Journal of Applied Earth Observation and Geoinformation, **58**, 177, **2017**.

57. LIU M., LIU X., LI M., FANG M., CHI W. Neural-network model for estimating leaf chlorophyll concentration in rice under stress from heavy metals using four spectral indices. Biosystems Engineering, **106** (3), 223, **2010**.

58. LI H.L., WANG Y.Y., AN S.Q., ZHI Y.B., LEI G.C., ZHANG M.X. Sediment type affects competition between a native and an exotic species in coastal China. Scientific Reports, **4**, 1, **2014**.

59. HOWARD R.J., BIAGAS J., ALLAIN L. Growth of Common Brackish Marsh Macrophytes Under Altered Hydrologic and Salinity Regimes. Wetlands, **36** (1), 11, **2016**.

60. MEDEIROS D.L., WHITE D.S., HOWES B.L. Replacement of Phragmites australis by Spartina alterniflora: The Role of Competition and Salinity. Wetlands, **33** (3), 421, **2013**.

61. SUTTER L.A., CHAMBERS R.M., PERRY J.E. Seawater intrusion mediates species transition in low salinity, tidal marsh vegetation. Aquatic Botany, **122**, 32, **2015**.

62. ZEREBECKI R.A., CRUTSINGER G.M., HUGHES A.R. Spartina alterniflora genotypic identity affects plant and consumer responses in an experimental marsh community. Journal of Ecology, **105** (3), 661, **2017**.

63. TUCKER C.J. Red and photographic infrared linear combinations for monitoring vegetation. Remote Sensing of Environment, **8** (2), 127, **1979**.

64. DAUGHTRY C.S.T., WALTHALL C.L., KIM M.S., DE COLSTOUN E.B., MCMURTREY J.E. Estimating Corn Leaf Chlorophyll Concentration from Leaf and Canopy Reflectance. Remote Sensing of Environment, **74** (2), 229, **2000**.

65. BROGE N.H., LEBLANC E. Comparing prediction power and stability of broadband and hyperspectral vegetation indices for estimation of green leaf area index and canopy chlorophyll density. Remote Sensing of Environment, **76** (2), 156, **2001**.

66. HABOUDANE D., MILLER J.R., PATTEY E., ZARCO-TEJADA P.J., STRACHAN I.B. Hyperspectral vegetation indices and novel algorithms for predicting green LAI of crop canopies: Modeling and validation in the context of precision agriculture. Remote Sensing of Environment, **90** (3), 337, **2004**.

67. GITELSON A.A., KAUFMAN Y.J., STARK R., RUNDQUIST D. Novel algorithms for remote estimation of vegetation fraction. Remote Sensing of Environment, **80** (1), 76, **2002**.

68. KIM M S., DAUGHTRY C.S. T., CHAPPELLE E.W., MCMURTREY J.E., WALTHALL C.L. The use of high spectral resolution bands for estimating absorbed photosynthetically active radiation (Apar). In Sixth Symposium on Physical Measurements and Signatures in Remote Sensing (pp. 299-306). ValD'Isere, France, **1994**.

69. HUETE A.R., LIU H.Q., BATCHILY K., VAN LEEUWEN, W. A comparison of vegetation indices over a global set of TM images for EOS-MODIS. Remote Sensing of Environment, **59** (3), 440, **1997**.

70. WU C., NIU Z., TANG Q., HUANG W. Estimating chlorophyll content from hyperspectral vegetation indices: Modeling and validation. Agricultural and Forest Meteorology, **148** (8-9), 1230, **2008**.

71. ROUJEAN J.L., BREON F.M. Estimating PAR absorbed by vegetation from bidirectional reflectance measurements. Remote Sensing of Environment, **51** (3), 375, **1995**.

72. VINCINI M., FRAZZI E., D'ALESSIO P. Angular dependence of maize and sugar beet Vis from directional CHRIS/PROBA data. ESRIN, Frascati, Italy: Fourth ESA CHRIS PROBA Workshop, **2006**.

73. HABOUDANE D., MILLER J.R., TREMBLAY N., ZARCO-TEJADA P.J., DEXTRAZE L. Integrated narrow-band vegetation indices for prediction of crop chlorophyll content for application to precision agriculture. Remote Sensing of Environment, **81** (2-3), 416, **2002**.

74. MUTANGA O., SKIDMORE A.K. Narrow band vegetation indices overcome the saturation problem in

biomass estimation. International Journal of Remote Sensing, **25** (19), 3999, **2004**.

75. LE MAIRE G., FRANÇOIS C., DUFRÊNE E. Towards universal broad leaf chlorophyll indices using PROSPECT simulated database and hyperspectral reflectance measurements. Remote Sensing of Environment, **89** (1), 1, **2004**.

76. LE MAIRE G., FRANÇOIS C., SOUDANI K., BERVEILLER D., PONTAILLER J.Y., BRÉDA N., DUFRÊNE E. Calibration and validation of hyperspectral indices for the estimation of broadleaved forest leaf chlorophyll content, leaf mass per area, leaf area index and leaf canopy biomass. Remote Sensing of Environment, **112** (10), 3846, **2008**.

77. CROFT H., CHEN J.M., ZHANG Y. The applicability of empirical vegetation indices for determining leaf chlorophyll content over different leaf and canopy structures. Ecological Complexity, **17** (1), 119, **2014**.

78. ZARCO-TEJADA P.J., PUSHNIK J.C., DOBROWSKI S., USTIN S.L. Steady-state chlorophyll a fluorescence detection from canopy derivative reflectance and double-peak red-edge effects. Remote Sensing of Environment, **84** (2), 283, **2003**.

79. SIMS D.A., GAMON J.A. Relationships between leaf pigment content and spectral reflectance across a wide range of species, leaf structures and developmental stages. Remote Sensing of Environment, **81** (2-3), 337, **2002**.

80. QI J., CHEHBOUNI A., HUETE A.R., KERR Y.H., SOROOSHIAN S. A modify soil adjust vegetation index. Remote Sensing of Environment, **126**, 119, **1994**.

81. CHEN J.M. Evaluation of Vegetation Indices and a Modified Simple Ratio for Boreal Applications. Canadian Journal of Remote Sensing, **22** (3), 229, **1996**.

82. DASH J., CURRAN P.J. The MERIS terrestrial chlorophyll index. International Journal of Remote Sensing, **25** (23), 5403, **2004**.

83. GUYOT G., FREDERIC B. Utilisation de la Haute Resolution Spectrale pour Suivre L'etat des Couverts Vegetaux. Proceedings of the 4th International Colloquium on Spectral Signatures of Objects in Remote Sensing Aussios, France, 18-22 January 1988, **287**, 279, **1988**.

84. PENUELAS J., FREDERIC B., FILELLA I. Semi-Empirical Indices to Assess Carotenoids/Chlorophyll-a Ratio from Leaf Spectral Reflectance. Photosynthetica, **31**, 221, **1995**.

85. GITELSON A.A., KAUFMAN Y.J., MERZLYAK M.N. Use of a green channel in remote sensing of global vegetation from EOS- MODIS. Remote Sensing of Environment, **58** (3), 289, **1996**.

86. VOGELMANN J.E., ROCK B.N., MOSS D.M. Red edge spectral measurements from sugar maple leaves. International Journal of Remote Sensing, **14** (8), 1563, **1993**.

87. BLACKBURN G.A. Quantifying chlorophylls and carotenoids at leaf and canopy scales: An evaluation of some hyperspectral approaches. Remote Sensing of Environment, **66** (3), 273, **1998**.

88. GITELSON A.A., GRITZ Y., MERZLYAK M. N. Relationships between leaf chlorophyll content and spectral reflectance and algorithms for non-destructive chlorophyll assessment in higher plant leaves. Journal of Plant Physiology, **160** (3), 271, **2003**.